Published in final edited form as:

Eur J Immunol. 2018 March ; 48(3): 532–542. doi:10.1002/eji.201746976.

Tumor conditions induce bone marrow expansion of granulocytic, but not monocytic, immunosuppressive leukocytes with increased CXCR2 expression in mice

Zhen Bian[1], **Lei Shi**[1], **Mahathi Venkataramani**[1], **Ahmed Mansour Abdelaal**[1,2], **Courtney Culpepper**[1], **Koby Kidder**[1], **Hongwei Liang**[1,3], **Ke Zen**[3], and **Yuan Liu**[1]

[1]Program of Cell and Molecular Immunology, Department of Biology & Center of Inflammation, Immunity and Infection, Georgia State University, Atlanta, GA, USA

[2]Faculty of Science, Zagazig University, Zagazig, Egypt

[3]School of Life Science, Nanjing University, Nanjing, China

Abstract

Myeloid-derived suppressor cells (MDSCs) promote tumor growth through, in part, inhibiting T-cell immunity. However, mechanisms underlying MDSC expansion and guidance of MDSCs toward the tumor microenvironment remain unclear. Employing Percoll density gradients, we separate bone marrow (BM) leukocytes from tumor-bearing mice into four density-increasing bands with myeloid leukocytes enriched in bands III and IV. Band III comprises monocytes and low-density granulocytes, both confirmed to be M-MDSCs and G-MDSCs, respectively, by displaying potent inhibition of T-cell proliferation. However, monocytes act as M-MDSCs not only under tumor conditions but also the healthy condition. In contrast, band IV contains non-inhibitory, mature granulocytes. Only band III G-MDSCs display significant expansion in mice bearing B16 melanoma, Lewis lung carcinoma, or MC38 colon carcinoma. The expanded G-MDSCs also show increased CXCR2 expression, which guides egress out of BM, and produce arginase-1 and ROS upon encountering antigen-activated T cells. Adoptive transfer assays demonstrate that both G-MDSCs and mature granulocytes infiltrate tumors, but only the former displays sustention and accumulation. Intratumoral administrations of granulocytes further demonstrate that G-MDSCs promote tumor growth, whereas mature granulocytes exert minimal effects, or execute powerful anti-tumor effects providing the presence of PMN activation mechanisms in the tumor microenvironment.

Keywords

Bone marrow PMN; Ly6C; Melanoma; Myeloid-derived suppressor cells; Myelopoiesis

Full correspondence: Dr. Yuan Liu, Center of Inflammation, Immunity & Infection, Center for Diagnostics & Therapeutics, & Program of Immunology & Molecular Cellular Biology, Department of Biology, Georgia State University, Atlanta, GA 30303, USA yliu@gsu.edu.

Conflict of interest: The authors have declared no financial or commercial conflict of interest.

Additional supporting information may be found in the online version of this article at the publisher's web-site

Introduction

The expansion of heterogeneous myeloid-derived suppressor cells (MDSCs) is associated with tumor progression through promoting an immune-tolerant and tumor-supportive host condition [1–3]. MDSCs are comprised of two populations, G-MDSCs and M-MDSCs, referring to myeloid leukocytes bearing either granulocytic markers or monocytic markers, respectively. Both G- and M-MDSCs have the capacity to inhibit immune-active T cells and, indeed, MDSC infiltration of secondary lymphoid organs (e.g. spleen and lymph nodes) and tumor microenvironments correlates with a reduction in T-cell numbers and T-cell-mediated anti-tumor activities [4, 5]. However, how tumor conditions alter myelopoiesis leading to MDSC expansion, as well as how MDSCs are guided toward T-cell zones, remain unresolved and are important subjects to investigate.

Derived from the same hematopoietic progenitors, MDSCs share many proteins with those in their akin lineage of non-suppressive myeloid leukocytes [4, 6], and the lack of specific markers or methods to distinguish MDSCs hinders studies that aim to address the above questions. In mice, Gr-1^{+}CD11b^{+} has been used to designate MDSCs [7–11], but these markers are not MDSC-specific, and are also expressed by other myeloid leukocytes especially non-suppressive granulocytes (polymorphonuclear leukocytes, PMN). In humans, progresses have been made to better separate peripheral MDSCs [12–14]; however, these successes provide only narrow possibilities for further mechanistic investigations, as human patients compared to animal models allow for very limited experimental research.

In this study, we developed a Percoll density gradient-based method that enables separation of MDSCs from non-inhibitory leukocytes in murine tumor models. Analyses of bone marrow myeloid compartments revealed an extensive expansion of G-MDSCs, but not M-MDSCs, along with tumor growth of B16 melanoma, Lewis lung carcinoma (LLC) and MC38 colon carcinoma. These G-MDSCs display a low cell density but increased expression of CXCR2, which facilitates their release from the bone marrow and trafficking to TCR-activated T cells and tumor environments. Interestingly, our experiments revealed that bone marrow monocytes are natural MDSCs and possess the ability to inhibit T cells irrespective of tumor conditions, whereas mature PMN, whose formation is not diminished by tumor conditions, display strong anti-tumor effects providing tumor microenvironments present PMN activation mechanisms.

Results

Percoll gradient separation of myeloid leukocytes and MDSC

C57BL6 mice implanted with B16, LLC or M38 tumors displayed significant expansion of CD11b^{+}Gr-1^{+} myeloid leukocytes, which consisted of Gr-1^{high}Ly6G^{+} granulocytes and Gr-1^{med}Ly6C^{high} monocytes, in the bone marrow, peripheral blood, and spleen (Supporting Information Fig. 1, A and B). Further assays con-firmed that CD11b^{+}Gr-1^{+} leukocytes from tumor-bearing mice strongly inhibit T-cell proliferation, confirming their immunosuppressive activity (Supporting Information Fig. 1C and D).

Since $CD11b^+Gr\text{-}1^+$ leukocytes were heterogeneous, containing not only two populations of MDSCs (G- and M-) but also mature PMN that were likely non-immunosuppressive [12, 15, 16], we devised Percoll density gradients to separate bone marrow leukocytes from mice bearing melanoma (*s. c.*). Five discontinuous densities were prepared, resembling the gradients previously used to isolate mature PMN from bone marrow [17–19]. As shown in Fig. 1A, gradient centrifugation separated bone marrow cells into four cellular bands, I, II, III, and IV, settled at the density interface of 5–40, 40–50, 50–60, and 60–70%, respectively. For healthy mice, percentages of bone marrow cells distributed in I, II, III and IV were approximately 15, 25, 25, and 35%, respectively. For tumor-bearing mice, the percentage in band III was increased to ~45%, resulting in relative reductions in I and II (the sum <25%); however, band IV remained unchanged (Table 1). The same Percoll density gradients were also used to separate bone marrow cells from mice with B16 lung metastasis (*i. v.*), LLC (*s. c.* or *i. v.*) or M38 (*s. c*); all showed significant expansion of band III and relative reduction of bands I and II, while band IV remained unchanged (Table 1).

Cell determination revealed that bands I and II contained $B220^+$ B lymphocytes (~40%), a fraction (<10%) of $Gr\text{-}1^{med}Ly6C^{high}$ monocytic cells, and small cells, likely progenitor or stroma cells, whereas bands III and IV were enriched with $CD11b^+Gr\text{-}1^+$ myeloid leukocytes (Fig. 1B). In particular, band IV was essentially all mature PMN (>95%), which were $Ly6G^+$ and displayed multi-segmented nuclei and high SSC values indicative of complex intracellular granular structures (Fig. 1C–E). Conversely, band III was a mixture of $Ly6C^{high}$ monocytic cells and $Ly6G^+$, immature granulocytic cells as indicated by their less segmented or band-shape nuclei and lower SSC values (Fig. 1C–E). Significantly, we found that band III $Ly6G^+$ granulocytes were the exclusive myeloid population that had undergone substantial expansion under tumor conditions, and was progressively increasing along with tumor development (Table 1, Fig. 1F). Despite the percentage of $Ly6C^{high}$ monocytes being relatively reduced in band III, this population, and also mature PMN in band IV, were not significantly changed under tumor conditions (Table 1, Fig. 1F). Similar Percoll density gradients were also tested with success to separate peripheral leukocytes from healthy humans and cancer patients (Fig. 1G and H).

Analyses of low density $Ly6G^+$ granulocytes in band III also found that these cells, compared to mature PMN in band IV, were expressing lower levels of surface Ly6G antigen and intracellular myeloperoxidase (MPO) (Fig. 2A). They also demonstrated much lower levels of gelatinase activity (Fig. 2B), as well as lower levels of phagocytosis toward *E. coli* (Fig. 2C). When treated with PMA, band III $Ly6G^+$ granulocytes produced lower levels of ROS than band IV mature PMN, albeit ROS levels were consistently 20–30% higher in tumor-bearing mice than in healthy mice (Fig. 2D).

Characterization of immunosuppressive capacity of separated leukocytes

We tested which bone marrow population separated by Percoll gradients had the capacity to inhibit T-cell proliferation, therefore containing MDSCs. For these experiments, splenic T cells were induced to proliferate by cell surface ligation of CD3 and CD28, and in this system, bone marrow leukocytes were added at the ratio of leukocytes: splenocytes = 1:4. As shown in Fig. 3A, no inhibition was exerted by leukocytes harvested from bands I, II and IV

(PMN); in contrast, leukocytes from band III, either of healthy or tumor mice, displayed strong inhibition at variable levels. As shown, while the band III leukocytes from tumor mice completely inhibited both CD4 and CD8 T-cell proliferation, those from healthy mice also displayed clear inhibition, albeit notably less potent.

Since band III contained a mixture of granulocytic and monocytic cells, further enrichment/separation of granulocytes by Ly6G selection was performed and produced a population of > 97% purity, the rest of which were majorly (~ 80%) Ly6C^{high} monocytes. Testing these separated populations found that the band III Ly6G^{+} granulocytes from tumor mice potently inhibited T-cell proliferation, whereas those from healthy mice had no effect (Fig. 3B and C). Surprisingly, testing band III Ly6C^{high} monocytes found that those from tumor mice or healthy mice displayed equally potent inhibition of T-cell proliferation (Fig. 3, B and C).

Further testing Ly6C^{high} monocytes and Ly6G^{+} granulocytes isolated from the peripheral blood produced the same results, showing that granulocytes only from tumor mice inhibited T-cell proliferation, whereas monocytes from any mice, healthy or bearing tumors, displayed potent inhibition (Fig. 3D). These results suggest that bone marrow-derived monocytes are natural M-MDSCs and possess innate inhibition toward T cells irrespective of tumor growth; differently, granulocytes gain suppressive or G-MDSC capacity only under tumor conditions. Analyses of myeloid leukocytes in the spleen also showed an expansion of Ly6G^{+} granulocytes and Ly6C^{high} monocytes in tumor mice, and both displayed inhibition of T-cell proliferation (Fig. 3E).

As arginase activity has been suggested to be instrumental for the immunosuppressive function of MDSCs [1, 20], we tested for leukocyte-specific arginase (arginase-1) in different bone marrow populations. To our surprise, no arginase-1 was detected in any leukocyte population isolated from bone marrow, even those from tumor mice. However, exposure to proliferating T cells induced arginase-1 expression in monocytic and granulocytic populations that displayed immunosuppressive activity. As shown in Fig. 3F, after co-incubation in the T-cell proliferation system for over 24 h, arginase-1 was expressed in band III Ly6G^{+} granulocytes from tumor mice and Ly6C^{high} monocytes from both healthy and tumor mice. No arginase-1 expression was detected in band IV mature PMN from any mice, or in band III Ly6G^{+} granulocytes from healthy mice. Incubation of monocytes or granulocytes with cultured B16 cells failed to induce arginase-1 expression. Therefore, inducible arginase-1 expression in different leukocytes correlates with their MDSC activities. Furthermore, we observed that band III Ly6G^{+} granulocytes (G-MDSCs) from tumor mice were producing ROS when exposed to proliferating T cells, while band IV mature PMN, as well as the same density granulocytes from healthy mice, did not (Fig. 3G), even though mature PMN had a higher capacity of ROS production upon PMA treatment (Fig. 2D).

Ly6G^{+} granulocytes in healthy and tumor mice

Since band III Ly6G^{+} granulocytes were the myeloid leukocytes that extensively expanded in tumor mice, we further characterized these cells. Compared to the same density granulocytes from healthy mice, those from tumor mice expressed a slightly lower level of CD11b (Fig. 4A). Other cell surface proteins that were reportedly increased on G-MDSCs

isolated from the peripheral blood or the spleen, including M-CSF receptor (CD115), IL-4 receptor (IL-4R) and CD244 [15, 21], showed no or only slight differences between granulocytes from healthy and tumor mice (Fig. 4A). CXCR4, the receptor critical for granulocyte retention in the bone marrow [22, 23], also showed similar expression in most of our tests, except in a few cases showing reduction on band III granulocytes from tumor mice. In contrast, the expression of CXCR2 was significantly increased on band III $Ly6G^+$ granulocytes from tumor mice compared to those from healthy mice (Fig. 4A). CXCR2 is the principle chemokine receptor responding to CXC chemokines (e.g. CXCL-1/2) and directs granulocytes to egress out of the bone marrow and into the circulation and inflammatory tissues [22–25]. In healthy mice (blue line) the CXCR2 expression level is generally low on immature granulocytes (band III), but increases when granulocytes mature (band IV) (also see [26, 27]). However, in tumor mice, the CXCR2 expression on band III granulocytes increased multiple folds (Fig. 4A). Further chemotaxis assays (ex vivo) confirmed that these granulocytes had gained increased responsiveness to CXC chemokines. As shown (Fig. 4B), compared to the same density granulocytes from healthy mice that showed only weak responses, the band III granulocytes from tumor mice demonstrated enhanced chemotaxis toward CXCL1 (KC), resulting in over 40% of cells transmigrating across transfilters in 60 min. The band IV mature PMN from either healthy or tumor mice also displayed effective chemotaxis with ~50% of applied PMN transmigrated. Granulocyte chemotaxis toward KC was blocked by SB225002, a CXCR2 antagonist [28].

Adoptive transfer experiments were performed to assess granulocyte infiltration in vivo toward tumor tissues. For these experiments, $Ly6G^+$ granulocytes of band III or IV from healthy and tumor-bearing mice were labeled with CMTMR (red) and CFSE (green), respectively, and were then mixed and transferred into recipient mice that bore B16 melanoma (Fig. 4C). Analyses of the recipient mice 6 h later observed a considerable number of transferred granulocytes recruited into melanoma tissues except when SB225002 was given (Fig. 4C and D). The infiltrated granulocytes were those from band III of tumor mice (G-MDSCs, green) and band IV (mature PMN) from either healthy or tumor mice. Further analyses after 18 h found that only band III granulocytes from tumor mice (G-MDSCs, green) remained in melanoma tissues, whereas mature PMN from either mice disappeared. These data suggest that both mature PMN and G-MDSCs infiltrate melanoma tissues; however, G-MDSCs stay longer and thus likely exert greater effects than mature PMN. Meanwhile, band III granulocytes from healthy mice (red), though not appearing in melanoma tissues, were homing to bone marrow (Fig. 4E and F). We also observed that treating B16 tumor mice with SB225002 significantly reduced tumor burden (Fig. 4G and H), and this effect of tumor suppression was associated with increased T cells and reduced granulocytes in tumor tissues (Fig. 4I).

Considering both G-MDSCs and mature PMN have the capacity to infiltrate melanoma, we further evaluated their effects on tumor growth. For these experiments, the isolated band III granulocytes (G-MDSCs) from tumor mice and band IV mature PMN (5×10^6 each, $>90\%$ purity) were intratumorally injected into B16 melanoma when the tumor sizes were about 100 mm^3. As shown (Fig. 5A), intratumoral injections of G-MDSCs significantly promoted B16 tumor growth, while injections of mature PMN had only minute effects. Analyses of tumor-infiltrating T cells found that the transfer of G-MDSCs, but not PMN, significantly

reduced (> 50%) T cells of both CD4 and CD8 in tumor tissues, a fact consistent with in vitro studies showing that G-MDSCs inhibited T cells while PMN did not (Fig. 5B).

The absence of tumor suppression by mature PMN was puzzling, given that likely the same cells (N1 neutrophils) have been reported to possess anti-tumor capacities [29–31]. We tested if the lack of PMN activation in tumor tissues could be the reason and performed intratumoral PMN activation. A mixture of PMN activation agents including PMA, zymosan, and fMLP were injected into the same tumors three minutes after the tumors were injected with PMN. As shown (Fig. 5D), this procedure of intratumoral activation of PMN resulted in drastic shrinkage of B16 melanoma, suggesting that PMN execute powerful anti-tumor effects providing the presence of PMN activation mechanisms intratumorally.

Discussion

Although myelopoiesis can be found in different organs such as the spleen, the bone marrow is the central place for myelopoiesis and thus is most likely the major location of MDSC production under cancer conditions. Despite this fact, studies of MDSCs in bone marrow compared to other places are less prevalent. In our studies, extensive expansions of $CD11b^{+}Gr1^{+}$ myeloid leukocytes have been observed in the bone marrow of tumor-bearing mice. These leukocytes, though frequently classified as MDSC in literature [1, 5, 9], are heterogeneous, containing populations of immunosuppressive M-MDSCs and G-MDSCs along with non-immunosuppressive leukocytes especially large numbers of mature granulocytes (PMN). These facts not only perplex the field of study aiming to delineate the mechanisms by which tumor conditions alter myelopoiesis and induce immunosuppressive leukocytes, but also become the critical barrier for developing therapeutic strategies that suppress MDSC while preserving PMN essential for innate immunity.

Herein, we successfully modified Percoll density gradient separation, a method previously used to isolate bone marrow mature PMN, to separate MDSCs, especially G-MDSCs from non-immunosuppressive PMN. This method surpasses $Ly6G^{+}$-based selection or other isolation methods reported in literature in which studies of G-MDSCs have more than likely used a mixture of G-MDSCs and PMN due to the fact that their isolation methods were not allowing proper separation. In addition to this study, Granot and colleagues [12] had also employed density gradients (Histopaque) to study granulocyte dynamics during tumor progression. Differing from our work which studied bone marrow myeloid compartments under tumor conditions developed in a C57BL/6 background, Granot's work analyzed peripheral granulocytes in the 4T1 mammary tumor model in a BALB/c background. Despite these differences, our results are in agreement with some of Granot's data, especially the results showing that low-density granulocytes were significantly expanded in tumor-bearing mice and that this expansion did not appear to affect the population of mature PMN formation.

In particular, in five tumor allograft models including B16, LLC and MC38 subcutaneous engraftments, B16 lung metastasis, and LLC lung carcinoma, we found that the low-density granulocytic population, which was later confirmed to be G-MDSCs, was extensively expanded in the bone marrow, and this expansion contributed to the majority of increased

$CD11b^{+}Gr\text{-}1^{+}$ myeloid leukocytes. In comparison, the population size of $Ly6C^{high}$ monocytes/M-MDSCs did not significantly change after mice bore tumors. As stated above, the expansion of G-MDSCs was also found to neither increase nor decrease the population of mature PMN, suggesting that G-MDSCs are not precursory of PMN and the two populations might be derived from different paths. Interestingly, Granot's work showed that mature PMN could lose cell density, along with potent anti-tumor effects, when the tumor condition progressed toward the late stage [12]. In conclusion, these studies suggest that G-MDSCs might be the most important immunosuppressive component supporting tumor growth. This suggestion is in line with various human cancer conditions studied thus far, including bladder cancer [14, 32], head and neck cancer [33], non-small cell lung cancer [34–36], gastric cancer [37, 38], pancreatic carcinoma [39, 40] etc. in which G-MDSCs have been reported to be expanded and the primary source of immunosuppression. This also agrees with the speculation that IL-33 inhibits G-MDSC expansion and function, thereby inhibiting tumor growth, without affecting M-MDSCs [41]. A reduction of G-MDSCs has also been reported in cancer patients with longer overall survival and those who had responded to various chemotherapies [34, 42, 43].

Moreover, our data show that tumor-induced G-MDSCs are distinct from regular immature granulocytes and mature PMN by the capacity to inhibit T cells, the capability to express arginase-1, the increased expression of CXCR2 (versus regular immature granulocytes), and a long lifespan after infiltrating tissues (versus mature PMN). As shown in this study, although G-MDSCs and regular immature granulocytes share some physical indices (e.g. cell density and SSC value) and appearance (non-segmented nucleus), the former express a higher level of CXCR2 and, as such, gain egress into the circulation and tumor tissues, whereas the latter with low CXCR2 are primarily restrained to the bone marrow. Therefore, G-MDSCs behave like true effector leukocytes, designated to be released and execute immunosuppressive function at a distance. Indeed, adoptive transfer of G-MDSCs, and also mature PMN, into tumor-bearing mice resulted in their fast tracking into tumor tissues; however, G-MDSCs exhibited a longer retention than PMN, and apparent tumor-growth promotion, whereas mature PMN had nearly no effect. These results not only denote G-MDSC-mediated protumoral effects supporting tumor microenvironments, but also point out that mere mobilization of PMN into tumor tissues may lead to only minimal anti-tumor effects. Mechanisms that activate PMN in the tumor, as articulated in our experiments, are needed in order for PMN-mediated tissue damage to proceed and confer tumor elimination. However, it is conceivable that tumor microenvironments, which have the ability to mask tumor cells/tissues as 'healthy self', may not naturally present mechanisms that activate PMN for tissue damage, or might even be imposing immunosuppressive mechanisms that suppress PMN activation, and these would be challenges for developing PMN-based anti-tumor therapies. Along this line, it is also necessary to carefully consider the use of CXCR2 antagonists, which block both G-MDSCs and mature PMN. Perhaps, these reagents should be used only when the benefits of depleting G-MDSCs outweigh disadvantages that include compromising innate immunity and the possible PMN-mediated anti-tumor effects. Despite that G-MDSCs appear to be effector cells, studies have demonstrated the possibility of converting G-MDSCs into PMN by GM-CSF in vitro [15], suggesting that regulating G-MDSC plasticity might still be possible.

Very interestingly, our study reveals that the bone marrow monocytes in C57BL6 mice are natural M-MDSCs. As shown, freshly isolated Ly6C^{high} monocytes from either healthy or tumor-bearing mice demonstrated similarly potent inhibition of T-cell proliferation. Differing from G-MDSCs, which are associated with tumor conditions, monocytes being M-MDSCs show slight differences between mice with and without tumor growth. The observation that M-MDSCs are present in healthy C57BL6 mice has also been reported by Slaney et al. [44], who explored monocyte-mediated immunosuppression to treat autoimmune condition. Perhaps, M-MDSC-conveyed immunosuppression is essential for controlling sporadically occurring, 'dysregulated' T-cell activation, thus preventing unwanted autoimmunity, and possibly this mechanism is exploited by tumors especially at the initial stage before systemic immunosuppression is fortified by G-MDSCs. Therefore, it is essential to understand if this "monocytes/M-MDSCs status" is dynamic and whether it can be altered, such as under conditions of infection, vaccination, and inflammation, in which T-cell proliferation and development of adaptive immunity are central to the pathophysiological processes.

Despite that previous studies have suggested that arginase-1 pertains to MDSC-mediated T-cell inhibition [20, 45, 46], our study of bone marrow MDSCs demonstrates that the enzyme expression is precluded in both M- and G- MDSCs prior to their exposure to TCR-activated T-cell proliferation. Testing different leukocyte populations also confirmed that arginase-1 expression, although requiring induction, is restricted to M/G-MDSCs, not in regular immature granulocytes and mature PMN that lack the immunosuppressive capacity. In addition, G-MDSCs, but not mature PMN, were observed to produce ROS after encountering proliferating T cells, which is consistent with the notion that ROS is a mechanism for G-MDSC-mediated immunosuppression [1, 6]. Together, these results indicate that bone marrow myelopoiesis undergoes critical reprogramming under tumor conditions, resulting in the expansion of G-MDSCs, a special population of granulocytic leukocytes that express unique transcriptional and translational profiles, allowing these cells to become the most prominent cancer supporter during tumor progression.

Materials and methods

Tumor mouse models

C57BL/6J mice (6–8 week, 20–22 g, the Jackson Laboratory) were engrafted (allograft) with B16 melanoma, LLC or MC38 carcinoma (each 2×10^5 cells in 100 μL PBS) subcutaneously (*s.c.*) or intravenously (*i.v.*); tumors were generally formed in 2–3 weeks. Tumor sizes measured by calipers were calculated as: $V = \pi/6 \times (\text{width})^2 \times (\text{length})$. B16 (B16F10), LLC and MC38 cells were obtained from American Type Culture Collection (ATCC)). To test CXCR2 antagonist, SB225002 (Selleckchem) was given intraperitoneally (*i.p.*, 1 mg/kg) along with or after tumor engraftment. To test leukocyte trafficking to tumors, bone marrow G-MDSCs or mature PMN (1×10^7 each), with or without labeling with 5-(and-6)-(((4-chloromethyl) benzoyl) amino) tetramethyl-rhodamine (CMTMR, red) or carboxyfluorescein diacetate suc-cinimidyl ester (CFSE, green), were administered (*i.v.)* into B16 melanoma-bearing mice in which tumors were about 500 mm^3, or injected intratumorally when the tumor size was about 100mm^3. In the latter experiments, immediate

injections of PMN activation agent, a mixture of PMA (1 μM), zymosan (0.25 mg) and fMLP (1 μM), in 50 μL PBS, was performed following the intratumoral PMN administration in a set of experiments.

Percoll density gradients separating leukocytes

Prior to preparing density gradients, Percoll (Sigma) was adjusted to 150 mM NaC1, 325 mOsM by mixing 1-part 10× HBSS with 9-parts Percoll. Further dilution in HBSS (v/v) produced Percoll density solutions of 80% (1.099 g/mL), 70% (1.088 g/mL), 60% (1.076 g/mL), 50% (1.064 g/mL), 40% (1.052 g/mL), and 5% (1.012 g/mL). Five-step discontinuous density gradients were prepared in a 15 mL tube by layering successively decreasing density solutions (2 mL/layer) upon one another (80, 70, 60, 50, 40, and 5%) starting with the densest placed at the bottom. To better distinguish density layers, some Percoll solutions were prepared in HBSS with phenol red to create alternating-colored density layers. About 5×10^7 bone marrow cells harvested from femur and tibia by flushing bone cavities and followed by RBC lysis were placed on top of the gradients in 2 mL PBS, followed by centrifugation at 1000 × *g* for 45 min in a swinging bucket rotor. This centrifugation did not disrupt Percoll density layers but resulted in cells forming bands at the density-transition interfaces. Cells in each band were collected, washed and analyzed by FACS. Further separation of $Ly6G^+$ granulocytic and $Ly6C^{high}$ monocytic cells enriched in band III was done using biotin-conjugated anti-Ly6G antibody and streptavidin-conjugated magnetic microbeads, which positively selected granulocytes (>95% purity), leaving the unbound to be majorly (>85%) of $Ly6C^{high}$ monocytes. Peripheral blood leukocytes were obtained after anticoagulation of the whole blood followed by RBC lysis prior to separation by Percoll gradients.

T-cell proliferation and inhibition assay

Fresh splenocytes (6×10^5) labeled with CFSE were induced to proliferate in a 96-well plate that had been immobilized with anti-CD3 antibody (1 μg/mL) in the presence of soluble anti-CD28 antibody (0.5 μg/mL, both from Biolegend) in RPMI1640 with 10% FBS for 4 days (37°C, 5% CO_2). To test inhibitory effects by myeloid leukocytes, different populations of leukocytes were added into the T-cell proliferation system at the ratio of 1:2, 1:4, or 1:8 of leukocytes to splenocytes. T-cell proliferation was then evaluated microscopically and by FACS that determined CFSE dilution.

PMN/granulocyte functional assays

To measure ROS production, leukocytes treated with 1 μM PMA or exposed to CD3/CD28-induced T-cell proliferation were in the presence of oxidation-sensitive dye DCFDA (5 μM, Invitrogen). After washing, DCFDA staining, which was correlated with ROS production intracellularly, was measured by FACS. To measure phagocytosis, leukocytes (1×10^6) were incubated with 1 μg Alexa Fluor 488-conjugated *E. coli* BioParticles (Invitrogen) at 37°C for 15 min. After washing, cells were further labeled for CD11b and/or Ly6G, or directly analyzed by FACS. Arginase-1 expression was detected by Western blot using an anti-arginase-1 antibody (H-52, Santa Cruz Biotechology) after granulocyte lysis. To measure gelatinase activity, gelatin zymography was performed using acrylamide gels embedded with 0.1% gelatin (Bio-Rad) following the manufacturer's protocol. To test chemotaxis, different

populations of granulocytes (2×10^6) were labeled with CFSE and then placed into the upper chambers of transwell devices containing collagen-coated transfilters (0.33 cm^2, 5 μm pore size) [47, 48] in 150 μL HBSS without or with the addition of SB225002 (100 nM). Chemotactic transmigration was induced by murine keratinocyte chemoattractant (KC, 50 ng/mL, Peprotech) in the lower chambers in 500 μL HBSS (37°C, 1h).

Statistical analysis

Data are presented as the mean ± SEM. Statistical differences/significance between data were assessed by the two-tailed Student's *t*-test for two groups or one-way ANOVA followed by Dunnett's Multiple Comparison test.

Supplementary Material

Refer to Web version on PubMed Central for supplementary material.

Acknowledgments

This work was supported, in part, by a grant from National Institutes of Health (AI106839) and a research scholar grant from the American Cancer Society.

Abbreviations

BM	bone marrow
BSA	bovine serum albumin
FBS	fetal bovine serum
HBSS	Hank's balanced salt solution
PB	peripheral blood
SP	spleen

References

1. Gabrilovich DI, Nagaraj S. Myeloid-derived suppressor cells as regulators of the immune system. Nat Rev Immunol. 2009; 9:162–174. [PubMed: 19197294]
2. Delano MJ, Scumpia PO, Weinstein JS, Coco D, Nagaraj S, Kelly-Scumpia KM, O'Malley KA, et al. MyD88-dependent expansion of an immature GR-1(+)CD11b(+) population induces T-cell suppression and Th2 polarization in sepsis. J Exp Med. 2007; 204:1463–1474. [PubMed: 17548519]
3. Cripps JG, Gorham JD. MDSC in autoimmunity. Int Immunopharmacol. 2011; 11:789–793. [PubMed: 21310255]
4. Talmadge JE, Gabrilovich DI. History of myeloid-derived suppressor cells. Nat Rev Cancer. 2013; 13:739–752. [PubMed: 24060865]
5. Youn JI, Nagaraj S, Collazo M, Gabrilovich DI. Subsets of myeloid-derived suppressor cells in tumor-bearing mice. J Immunol. 2008; 181:5791–5802. [PubMed: 18832739]
6. Gabrilovich DI, Ostrand-Rosenberg S, Bronte V. Coordinated regulation of myeloid cells by tumours. Nat Rev Immunol. 2012; 12:253–268. [PubMed: 22437938]
7. Lin Y, Yang X, Liu W, Li B, Yin W, Shi Y, He R. Chemerin has a protective role in hepatocellular carcinoma by inhibiting the expression of IL-6 and GM-CSF and MDSC accumulation. Oncogene. 2017; 36:3599–3608. [PubMed: 28166197]

8. Kusmartsev SA, Li Y, Chen SH. Gr-1+ myeloid cells derived from tumor-bearing mice inhibit primary T-cell activation induced through CD3/CD28 costimulation. J Immunol. 2000; 165:779–785. [PubMed: 10878351]
9. Bronte V, Brandau S, Chen SH, Colombo MP, Frey AB, Greten TF, Mandruzzato S, et al. Recommendations for myeloid-derived suppressor cell nomenclature and characterization standards. Nat Commun. 2016; 7:12150. [PubMed: 27381735]
10. Song X, Krelin Y, Dvorkin T, Bjorkdahl O, Segal S, Dinarello CA, Voronov E, et al. $CD11b^{+}$/$Gr\text{-}1^{+}$immature myeloid cells mediate suppression of T cells in mice bearing tumors of IL-1β-secreting cells. J Immunol. 2005; 175:8200–8208. [PubMed: 16339559]
11. Huang B, Pan PY, Li Q, Sato AI, Levy DE, Bromberg J, Divino CM, et al. Gr-1+CD115+ immature myeloid suppressor cells mediate the development of tumor-induced T regulatory cells and T-cell anergy in tumor-bearing host. Cancer Res. 2006; 66:1123–1131. [PubMed: 16424049]
12. Sagiv JY, Michaeli J, Assi S, Mishalian I, Kisos H, Levy L, Damti P, et al. Phenotypic diversity and plasticity in circulating neutrophil subpopulations in cancer. Cell Reports. 2015; 10:562–573. [PubMed: 25620698]
13. Dumitru CA, Moses K, Trellakis S, Lang S, Brandau S. Neutrophils and granulocytic myeloid-derived suppressor cells: immunophenotyping, cell biology and clinical relevance in human oncology. Cancer Immunol Immunother. 2012; 61:1155–1167. [PubMed: 22692756]
14. Brandau S, Trellakis S, Bruderek K, Schmaltz D, Steller G, Elian M, Suttmann H, et al. Myeloid-derived suppressor cells in the peripheral blood of cancer patients contain a subset of immature neutrophils with impaired migratory properties. J Leukoc Biol. 2011; 89:311–317. [PubMed: 21106641]
15. Youn JI, Collazo M, Shalova IN, Biswas SK, Gabrilovich DI. Characterization of the nature of granulocytic myeloid-derived suppressor cells in tumor-bearing mice. J Leukocyte Biol. 2012; 91:167–181. [PubMed: 21954284]
16. Tsiganov EN, Verbina EM, Radaeva TV, Sosunov VV, Kosmiadi GA, Nikitina IY, Lyadova IV. Gr-1(dim)CD11b(+) immature myeloid-derived suppressor cells, but not neutrophils, are markers of lethal tuberculosis infection in mice. J Immunol. 2014; 192:4718–4727. [PubMed: 24711621]
17. Bian Z, Guo Y, Ha B, Zen K, Liu Y. Regulation of the inflammatory response: enhancing neutrophil infiltration under chronic inflammatory conditions. J Immunol. 2012; 188:844–853. [PubMed: 22156344]
18. Zen K, Guo Y, Bian Z, Lv Z, Zhu D, Ohnishi H, Matozaki T, et al. Inflammation-induced proteolytic processing of the SIRPalpha cytoplasmic ITIM in neutrophils propagates a proinflammatory state. Nat Commun. 2013; 4:2436. [PubMed: 24026300]
19. Dong X, Wu D. Methods for studying neutrophil chemotaxis. Methods Enzymol. 2006; 406:605–613. [PubMed: 16472691]
20. Zea AH, Rodriguez PC, Atkins MB, Hernandez C, Signoretti S, Zabaleta J, McDermott D, et al. Arginase-producing myeloid suppressor cells in renal cell carcinoma patients: a mechanism of tumor evasion. Cancer Res. 2005; 65:3044–3048. [PubMed: 15833831]
21. Mandruzzato S, Solito S, Falisi E, Francescato S, Chiarion-Sileni V, Mocellin S, Zanon A, et al. IL4Ralpha+ myeloid-derived suppressor cell expansion in cancer patients. J Immunol. 2009; 182:6562–6568. [PubMed: 19414811]
22. Martin C, Burdon PCE, Bridger G, Gutierrez-Ramos JC, Williams TJ, Rankin SM. Chemokines acting via CXCR2 and CXCR4 control the release of neutrophils from the bone marrow and their return following senescence. Immunity. 2003; 19:583–593. [PubMed: 14563322]
23. Eash KJ, Greenbaum AM, Gopalan PK, Link DC. CXCR2 and CXCR4 antagonistically regulate neutrophil trafficking from murine bone marrow. J Clin Investig. 2010; 120:2423–2431. [PubMed: 20516641]
24. Sadik CD, Kim ND, Luster AD. Neutrophils cascading their way to inflammation. Trends Immunol. 2011; 32:452–460. [PubMed: 21839682]
25. Katoh H, Wang D, Daikoku T, Sun H, Dey SK, Dubois RN. CXCR2-expressing myeloid-derived suppressor cells are essential to promote colitis-associated tumorigenesis. Cancer Cell. 2013; 24:631–644. [PubMed: 24229710]

26. Lloyd AR, Biragyn A, Johnston JA, Taub DD, Xu L, Michiel D, Sprenger H, et al. Granulocyte-colony stimulating factor and lipopolysaccharide regulate the expression of interleukin 8 receptors on polymorphonuclear leukocytes. J Biological Chem. 1995; 270:28188–28192.
27. Theilgaard-Mönch K, Jacobsen LC, Borup R, Rasmussen T, Bjer-regaard MD, Nielsen FC, Cowland JB, et al. The transcriptional program of terminal granulocytic differentiation. Blood. 2005; 105:1785–1796. [PubMed: 15514007]
28. White JR, Lee JM, Young PR, Hertzberg RP, Jurewicz AJ, Chaikin MA, Widdowson K, et al. Identification of a potent, selective non-peptide CXCR2 antagonist that inhibits interleukin-8-induced neutrophil migration. J Biol Chem. 1998; 273:10095–10098. [PubMed: 9553055]
29. Fridlender ZG, Sun J, Kim S, Kapoor V, Cheng G, Ling L, Worthen GS, et al. Polarization of tumor-associated neutrophil (TAN) phenotype by TGF-β: "N1" versus "N2" TAN. Cancer Cell. 2009; 16:183–194. [PubMed: 19732719]
30. Droeser RA, Hirt C, Eppenberger-Castori S, Zlobec I, Viehl CT, Frey DM, Nebiker CA, et al. High myeloperoxidase positive cell infiltration in colorectal cancer is an independent favorable prognostic factor. PLoS One. 2013; 8:e64814. [PubMed: 23734221]
31. Zilio S, Serafini P. Neutrophils and granulocytic MDSC: the janus god of cancer immunotherapy. Vaccines (Basel). 2016; 4:31.
32. Eruslanov E, Neuberger M, Daurkin I, Perrin GQ, Algood C, Dahm P, Rosser C, et al. Circulating and tumor-infiltrating myeloid cell subsets in patients with bladder cancer. Int J Cancer. 2012; 130:1109–1119. [PubMed: 21480223]
33. Corzo CA, Cotter MJ, Cheng P, Cheng F, Kusmartsev S, Sotomayor E, Padhya T, et al. Mechanism regulating reactive oxygen species in tumor induced myeloid-derived suppressor cells: MDSC and ROS in cancer. J Immunol. 2009; 182:5693–5701. [PubMed: 19380816]
34. Liu CY, Wang YM, Wang CL, Feng PH, Ko HW, Liu YH, Wu YC, et al. Population alterations of L-arginase-and inducible nitric oxide synthase-expressed CD11b+/CD14(−)/CD15+/CD33+ myeloid-derived suppressor cells and CD8+ T lymphocytes in patients with advanced-stage non-small cell lung cancer. J Cancer Res Clin Oncol. 2010; 136:35–45. [PubMed: 19572148]
35. Heuvers ME, Muskens F, Bezemer K, Lambers M, Dingemans AM, Groen HJ, Smit EF, et al. Arginase-1 mRNA expression correlates with myeloid-derived suppressor cell levels in peripheral blood of NSCLC patients. Lung Cancer. 2013; 81:468–474. [PubMed: 23850196]
36. Koinis F, Vetsika EK, Aggouraki D, Skalidaki E, Koutoulaki A, Gkioulmpasani M, Georgoulias V, et al. Effect of first-line treatment on myeloid-derived suppressor cells' subpopulations in the peripheral blood of patients with non-small cell lung cancer. J Thorac Oncol. 2016; 11:1263–1272. [PubMed: 27178984]
37. Wang L, Chang EW, Wong SC, Ong SM, Chong DQ, Ling KL. Increased myeloid-derived suppressor cells in gastric cancer correlate with cancer stage and plasma S100A8/A9 proinflammatory proteins. J Immunol. 2013; 190:794–804. [PubMed: 23248262]
38. Zhang B, Wang Z, Wu L, Zhang M, Li W, Ding J, Zhu J, et al. Circulating and tumor-infiltrating myeloid-derived suppressor cells in patients with colorectal carcinoma. PLoS One. 2013; 8:e57114. [PubMed: 23437326]
39. Porembka MR, Mitchem JB, Belt BA, Hsieh CS, Lee HM, Herndon J, Gillanders WE, et al. Pancreatic adenocarcinoma induces bone marrow mobilization of myeloid-derived suppressor cells which promote primary tumor growth. Cancer Immunol Immunother. 2012; 61:1373–1385. [PubMed: 22215137]
40. Khaled YS, Ammori BJ, Elkord E. Increased levels of granulocytic myeloid-derived suppressor cells in peripheral blood and tumour tissue of pancreatic cancer patients. J Immunol Res. 2014; 2014:879–897.
41. Xiao P, Wan X, Cui B, Liu Y, Qiu C, Rong J, Zheng M, et al. Interleukin 33 in tumor microenvironment is crucial for the accumulation and function of myeloid-derived suppressor cells. Oncoimmunology. 2016; 5:e1063772. [PubMed: 26942079]
42. Christiansson L, Soderlund S, Svensson E, Mustjoki S, Bengtsson M, Simonsson B, Olsson-Stromberg U, et al. Increased level of myeloid-derived suppressor cells, programmed death receptor ligand 1/programmed death receptor 1, and soluble CD25 in Sokal high risk chronic myeloid leukemia. PLoS One. 2013; 8:e55818. [PubMed: 23383287]

43. Ko JS, Zea AH, Rini BI, Ireland JL, Elson P, Cohen P, Golshayan A, et al. Sunitinib mediates reversal of myeloid-derived suppressor cell accumulation in renal cell carcinoma patients. Clin Cancer Res. 2009; 15:2148–2157. [PubMed: 19276286]

44. Slaney CY, Toker A, La Flamme A, Backstrom BT, Harper JL. Naive blood monocytes suppress T-cell function. A possible mechanism for protection from autoimmunity. Immunol Cell Biol. 2011; 89:7–13. [PubMed: 21060323]

45. Vasquez-Dunddel D, Pan F, Zeng Q, Gorbounov M, Albesiano E, Fu J, Blosser RL, et al. STAT3 regulates arginase-I in myeloid-derived suppressor cells from cancer patients. J Clin Investig. 2013; 123:1580–1589. [PubMed: 23454751]

46. Rodriguez PC, Ernstoff MS, Hernandez C, Atkins M, Zabaleta J, Sierra R, Ochoa AC. Arginase I-producing myeloid-derived suppressor cells in renal cell carcinoma are a subpopulation of activated granulocytes. Cancer Res. 2009; 69:1553–1560. [PubMed: 19201693]

47. Liu Y, Merlin D, Burst SL, Pochet M, Madara JL, Parkos CA. The role of CD47 in neutrophil transmigration. Increased rate of migration correlates with increased cell surface expression of CD47. J Biol Chem. 2001; 276:40156–40166. [PubMed: 11479293]

48. Zen K, Reaves TA, Soto I, Liu Y. Response to genistein: Assaying the activation status and chemotaxis efficacy of isolated neutrophils. J Immunolog Methods. 2006; 309:86–98.

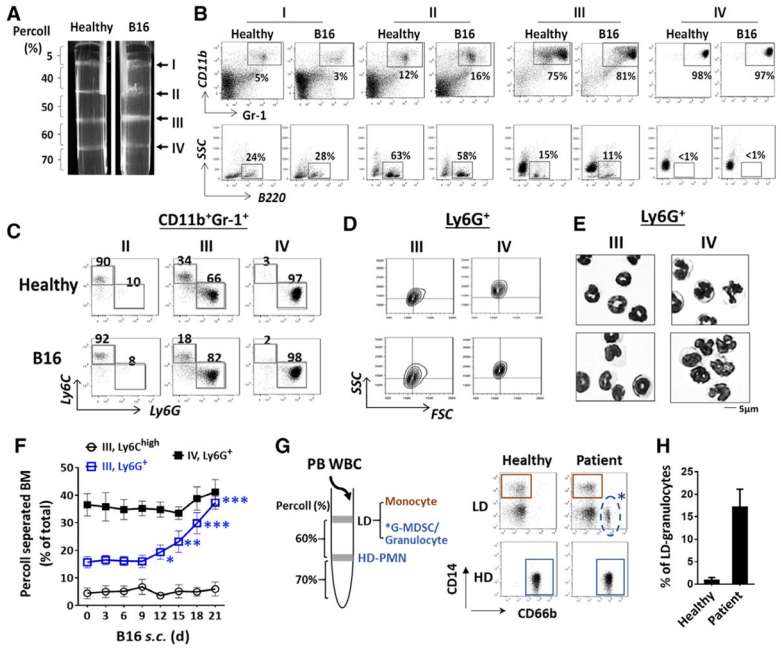

Figure 1.

Separation of bone marrow myeloid leukocytes by Percoll density gradients. **(A)** Bone marrow cells harvested from healthy and B16 melanoma-bearing mice were applied to discontinuous Percoll density gradients. After centrifugation, four cell-enriched bands, I, II, III, IV, were formed at sequentially increased density interfaces. Representative flow cytometric **(B)** analyses of cell types in each band. **(C)** Determination of monocytic and granulocytic cells in the Gr-1$^+$CD11b$^+$ myeloid population by Ly6C and Ly6G labeling. **(D)** Analyses of Ly6G$^+$ granulocytes in bands III and IV for FSC and SSC values. **(E)** Giemsa staining of Ly6G$^+$ granulocytes for nuclear morphology. Scale bar: 5 μm. Data in (A–E) are from a single experiment representative of over five independent experiments with three to five mice per experiment. **(F)** Progressive expansion of band III Ly6G$^+$ granulocytes in mice engrafted with B16 melanoma. **(G–H)** Separation of human peripheral leukocytes by Percoll density gradients and FACS analyses of granulocytes (CD66$^+$) and monocytes (CD14$^+$) in high density (HD) and low density (LD) fractions. Data in (F, H) are expressed as median ± SEM and represent over five independent experiments with five mice or patients per experiment. The significant differences between the tested groups were calculated by two-tailed paired Student's *t*-test. *$p \leq 0.05$; **$p \leq 0.01$; ***$p \leq 0.001$.

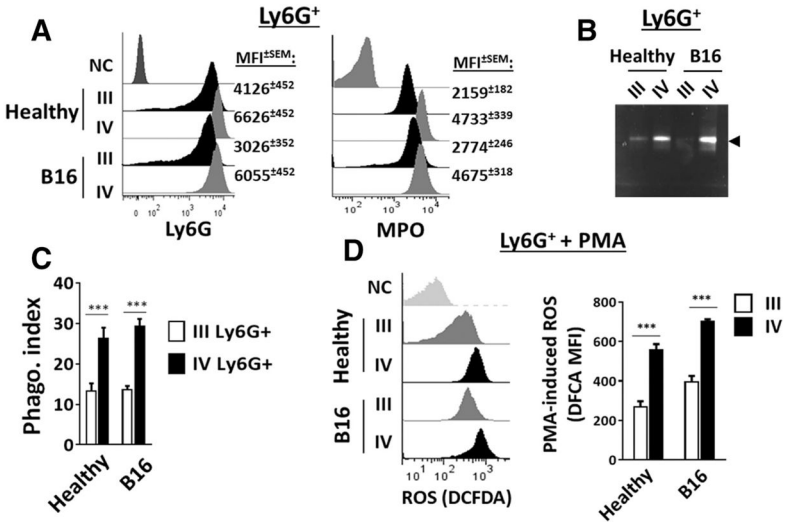

Figure 2.

Functional characterization of Ly6G$^+$ granulocytes in bands III and IV. **(A)** Expression of cell surface Ly6G antigen and intracellular MPO. Ly6G$^+$ granulocytes in bands III and IV were directly incubated with an anti-Ly6G antibody to detect cell surface Ly6G or were first permeabilized using Triton prior to incubation with PE-conjugated anti-MPO antibody for MPO detection by flow cytometry. NC: Cells labeled with PE-conjugated goat anti-rat IgG. **(B)** PMA-induced release of gelatinase activity. The supernatants of PMA-treated Ly6G$^+$ granulocytes were collected and gelatinase activity (arrowhead) was analyzed by zymography. **(C)** Phagocytosis toward Alexa Fluor-conjugated *E. coli*. **(D)** PMA-induced ROS production determined by DCFDA staining. Data demonstrated in C and D are expressed as median ± SEM and represent over five independent experiments with over five mice per experiment. The significant differences between the tested groups were calculated by two-tailed paired Student's *t*-test. ***$p \leq 0.001$. Data demonstrated in (A, B and left panel of D) are from a single experiment representative of five independent experiments with at least three mice per experiment.

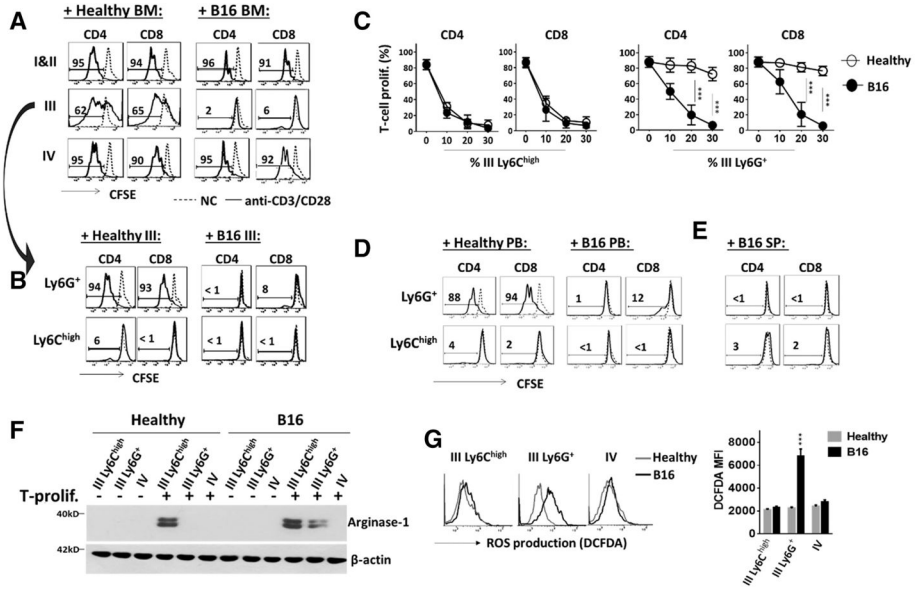

Figure 3.

MDSC activity in different myeloid populations. **(A)** Assay for bone marrow leukocyte-mediated inhibition of T-cell proliferation. Splenic T cells (labeled with CFSE) were induced for proliferation by ligating CD3 and CD28 followed by incubation at 37°C. After 4 days, positive proliferation was determined by the CFSE dilution toward a lower fluorescence intensity. To test leukocytes-mediated inhibition, bone marrow leukocytes from healthy and B16 melanoma mice separated by Percoll gradients in bands I and II (combined), III, and IV were added into the T-cell proliferation system at the ratio of 1:4 for leukocytes to splenocytes. **(B)** Inhibition of T-cell proliferation by band III Ly6G$^+$ granulocytes and Ly6C^{high} monocytes. Ly6G selection was performed to separate the band III granulocytes from monocytes prior to testing both cell types in T-cell proliferation assays. **(C)** Dose-dependent inhibition of proliferation by band III Ly6G$^+$ granulocytes and Ly6C^{high} monocytes. **(D and E)** Testing Ly6G$^+$ granulocytes and Ly6C^{high} monocytes from peripheral blood (PB) and spleen (SP) for inhibition of T-cell proliferation. **(F)** Western blot detecting arginase-1 in band III and IV bone marrow leukocytes before (−) and after (+) co-culturing these cells with CD3/CD28-ligated T cells. **(G)** Induced ROS production in G-MDSCs by proliferating T cells. The band III and IV bone marrow leukocytes from different mice were co-cultured with CD3/CD28-ligated T cells in the presence of DCFDA for 6 h. ROS production indicated by positive DCFDA staining was evaluated by flow cytometry. Flow cytometry data in A, B, D, G are from one experiment representative of at least three experiments with over six mice per experiment. Statistical data in C and G are expressed as median ± SEM and represent at least three experiments with over six mice per experiment. The significant differences between the tested groups were calculated by two-tailed paired Student's *t*-test. ***$p \leq 0.001$.

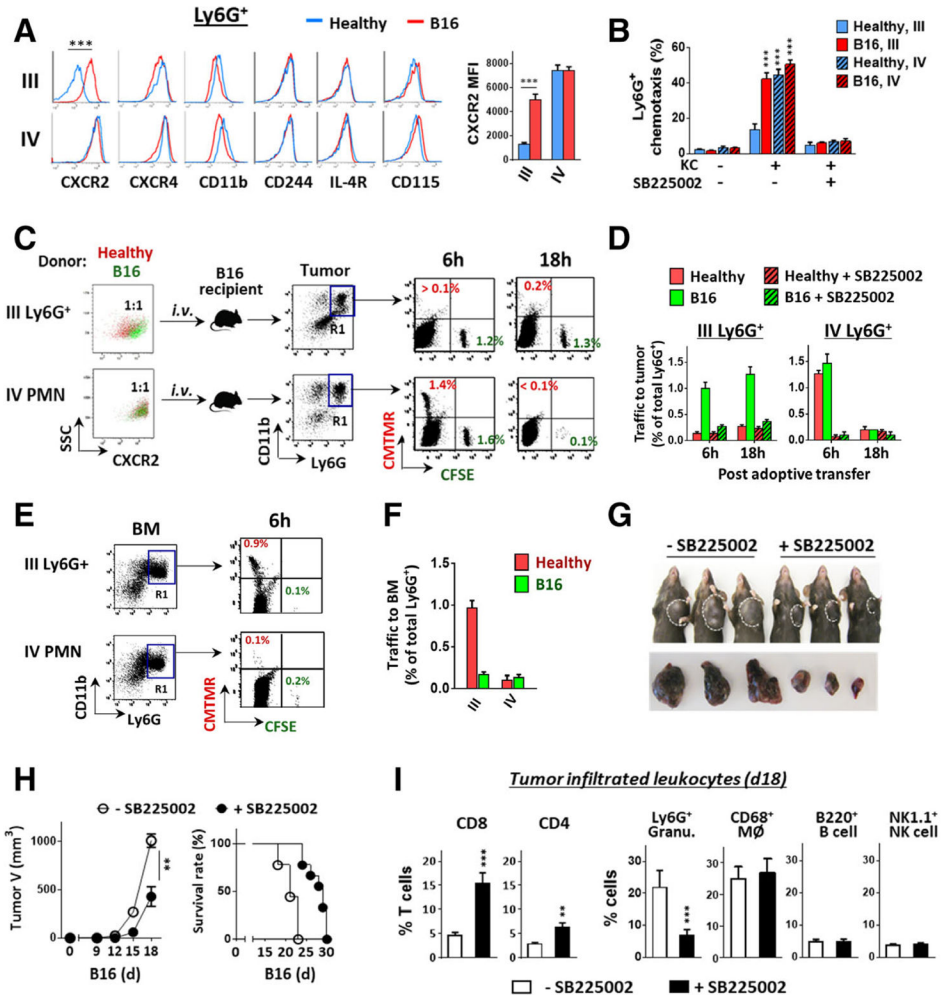

Figure 4.

Increased CXCR2 expression on G-MDSCs directs egress out of bone marrow into tumors. **(A)** Isolated bone marrow band III and IV Ly6G$^+$ granulocytes from healthy and melanoma-bearing mice were detected for cell surface markers by flow cytometry. **(B)** G-MDSC and PMN chemotaxis toward CXCL1 (KC). In vitro chemotaxis assays were performed using transwell setups toward KC in the presence or absence of a CXCR2 antagonist SB225002). **(C–F)** In vivo granulocyte trafficking to B16 melanoma. Isolated band III Ly6G$^+$ granulocytes and band IV mature PMN were labeled with fluorescence dye, CMTMR (red) for those originated from healthy mice, or CFSE (green) for those originated from melanoma-bearing mice. Mixed red and green (1:1 ratio) granulocytes of band III or IV were then transferred *i.v.* into melanoma-bearing recipient mice (tumor size ~ 500 mm^3), without or along with SB225002. At 6 and 18 h post transfer, melanoma tumors (C and D) and femur bones (E–F) were excised and analyzed for colored granulocytes within CD11b $^+$Ly6G$^+$ cells (R1 gating), indicating donor Ly6G$^+$ granulocyte trafficking. **G–I)**. Mice engrafted with B16 were given (*i.p.*, 3×) SB225002 or vehicle every other day. The effects on tumor growth (G and H), the overall survival rates (H), and the intratumoral T cells and other leukocytes (I) were determined on day 18. Flow data in left panel A, C and E are from

a single experiment representative of at least three independent experiments with five mice per experiment. Data in A, B, D, F, H and I are presented as mean ± SEM and represent at least three experiments with more than five mice per experiment. The significant differences between the tested groups were calculated by two-tailed paired Student's *t*-test (A, H, I) or one-way ANOVA followed by Dunnett's Multiple Comparison test (B). $^{**}p \leq 0.01$; $^{***}p \leq 0.001$.

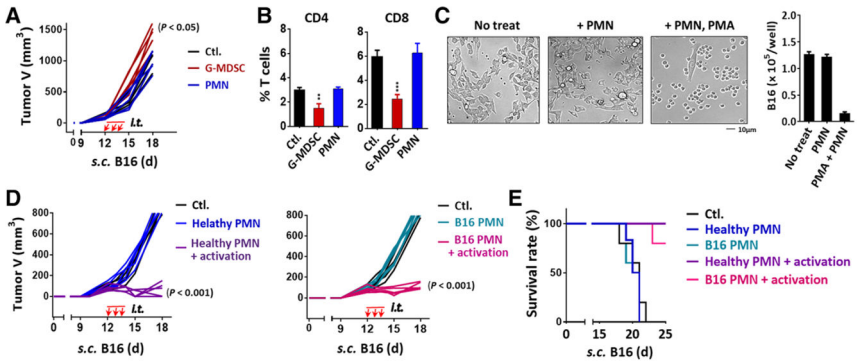

Figure 5.

Effects of G-MDSCs and mature PMN on tumor growth. **(A and B)** Isolated G-MDSCs or PMN from bone marrow bands III and IV of melanoma-bearing mice were intratumorally injected (i.t.) into recipient mice that bore melanoma tumors (tumor size ~ 100 mm^3) for three consecutive days (days 12, 13, and 14). Tumor growth was recorded (A) and tumor infiltrated T cells were analyzed on day 15 (B). **(C)** B16 cells were co-cultured with PMN in the absence or presence of PMA for 18 h. **(D and E)** Bone marrow PMN (band IV) isolated from healthy or tumor-bearing mice were intratumorally injected into recipient melanoma tumors. To activate PMN, a set of mice were given the second injections of a mixture of PMA, zymosan and fMLP. These procedures were performed three times (d 12, 13, and 14). Tumor growth (D) and the overall survival rates (E) were analyzed. Demonstrated data (A–D) represent at least three independent experiments with five or six mice per experiment. Data in B and C are presented as mean ± SEM. The significant differences between the tested groups were calculated by one-way ANOVA followed by Dunnett's Multiple Comparison test. *$p \leq 0.05$; **$p \leq 0.01$; ***$p \leq 0.001$.

Table 1

Percoll-density separation of bone marrow (BM) cells

	Percoll density separated BM cells (% of total) (Mean ± SEM)					
Band	Healthy ($n = 6$)	B16 (s.c.) ($n = 5$)	B16 (i.v.) ($n = 4$)	LLC (s.c.) ($n = 5$)	LLC (i.v.) ($n = 4$)	MC38 (s.c.) ($n = 5$)
I	17.4 ± 3.0	7.9 ± 2.2	9.3 ± 1.5	6.8 ± 2.5	10.4 ± 1.6	9.4 ± 1.0
II	24.7 ± 2 .3	15.0 ± 2.3	13.7 ± 1.5	13.0 ± 2.0	14.1 ± 2.3	14.0 ± 2.7
III	26.8 ± 2.4	45.2 ± 5.5[a)]	41.7 ± 3.1[a)]	42.7 ± 2.9[a)]	46.2 ± 4.2[a)]	45.4 ± 4.9[a)]
ly6C^{high}	6.4 ± 1.1	8.3 ± 1.3	8.0 ± 0.6	7.9 ± 1.2	7.6 ± 2.5	8.8 ± 1.7
ly6G^{+}	12.4 ± 1.7	27.1 ± 3.5[a)]	25.4 ± 2.4[a)]	28.6 ± 2.8[a)]	28.1 ± 3.2[a)]	25.2 ± 2.9[a)]
IV	31.1 ± 3.8	30.9 ± 2.8	33.3 ± 3.0	34.5 ± 3.4	30.3 ± 2.9	31.2 ± 4.5
Total BM cells (x10^6)	30.2 ± 3.3	36.6 ± 4.4	34.1 ± 3.7	36.9 ± 4.2	35.8 ± 3.2	37.1 ± 2.4

BM from healthy mice and mice engrafted with B16 melanoma, LLC lung carcinoma or MC38 colon cancer for 21 days were harvested from femur and tibia bones, followed by separation by Percoll density gradients. Total BM cells prior to separation and cells distributed in bands I to IV were counted. Ly6C^{high} and Ly6G^{+} cells in band III were determined by FACS. The significant differences between the tested groups were calculated by one-way ANOVA followed by Dunnett's Multiple Comparison test.

a) $p \leq 0.001$